are in fact equivalent since they produce identical reduced-order models. In particular,

1. The formulations of Davison (1966) and Nicholson (1964) are equivalent.
2. Marshall's method (1966) and one of Chidambara's proposed methods (Chidambara and Davison, 1967b) are equivalent, as previously noted by Graham (1968).
3. The approaches of Fossard (1970) and Graham (1968) are equivalent to a revision of Davison's method derived by Chidambara and Davison (1967b).

Proofs that the resulting reduced-order models are equivalent were developed as part of this investigation and are available elsewhere (Wilson, 1974).

Manuscript received October 24, 1973; revision received July 15 and accepted July 16, 1974.

Developing and Fully Developed Velocity Profiles for Inelastic Power Law Fluids in an Annulus

Developing and fully developed velocity profiles with respect to position for laminar flow of inelastic fluids in an annulus were measured using streak photography. The polymer solutions used in the investigation were found to exhibit power law behavior under the present experimental conditions. The experimental results substantiated published theoretical solutions for developing and fully developed flow of power-law fluids in annuli, and also indicated good agreement between the measured and predicted entrance lengths. The dimensionless entrance length was found to increase with increasing flow behavior index for the inelastic power-law fluids.

CARLOS TIU

and

SATINATH BHATTACHARYYA

Department of Chemical Engineering
Monash University
Clayton, Victoria 3168, Australia

SCOPE

Developing and fully developed laminar flow of non-Newtonian fluids in annuli is of importance in many industrial applications such as in heat transfer, in plastic extrusion, in mixing of viscous liquids, and in well bore fluid circulation. Experimental work in this area of research, particularly the entry flow problem, is almost nonexistent. When a fluid enters an annulus through a contraction, it undergoes a change in the flow pattern from an initial velocity profile at the inlet to a fully developed profile at a certain distance downstream. Associated with the developing field is an increase in kinetic energy and in viscous friction, which results in a higher pressure drop in the entrance region. Hence, quantitative information on entrance length, defined as the distance from the inlet to the point of fully developed flow, is of importance to the design or process engineer. Although most highly viscous non-Newtonian fluids are also elastic in nature, an understanding of the inelastic flow behavior in an annular entry is essential before the more complicated viscoelastic problem can be tackled. In the present study experimental measurements of developing and fully developed velocity profiles in an annulus are presented for some inelastic polymer solutions. The measured profiles are used to compare and substantiate published theoretical solutions. The entrance lengths in the annulus are established from the developing velocity profiles.

CONCLUSIONS AND SIGNIFICANCE

The significance of the present work lies in the accurate photographic measurements of velocity distributions for the laminar flow of non-Newtonian fluids in an annulus. The theoretical fully developed velocity profiles obtained from the solution of Fredrickson and Bird (1958) for the flow of power-law fluids in annuli were substantiated for the first time with the present experimental measurements. The measured developing velocity profiles for inelastic fluids in the entrance region showed excellent agreement with the momentum-energy integral solution published previously by the authors (1973). Therefore, a quantitative estimate of the entrance length in an annulus can

S. Bhattacharyya is with the Melbourne Metropolitan Board of Works, Melbourne, Victoria, Australia.

be achieved. The dimensionless entrance length for the flow of inelastic power-law fluids in an annulus was found to increase with increasing flow behavior index. A small vena contracta was detected immediately downstream of the annular contraction, but its presence had no significant effect on the velocity profile measurements.

A number of theoretical solutions for fully developed flow of various non-Newtonian model fluids in annuli have been published (Fredrickson and Bird, 1958; Rotem, 1962; McEachern, 1966; Kozicki et al., 1966, 1971). However, experimental investigations on non-Newtonian annular flow are scarce. There appear to be no velocity profile measurements, either developing or fully developed, for non-Newtonian flow in annuli reported in the literature. In two previous papers (Tiu and Bhattacharyya, 1973, 1974) theoretical solutions and experimental pressure profiles for the flow of power-law fluids in the entrance region of annuli have been reported. In this work experimental measurements of the developing and fully developed velocity profiles for inelastic power-law fluids in an annulus will be presented and used to substantiate prior works.

When a fluid in laminar motion enters an annulus through an abrupt contraction, the velocity distribution undergoes a development from an initial profile at the inlet, usually assumed uniform or flat, to a fully developed profile at some distance downstream of the contraction. The axial distance, usually in dimensionless form $x/r_H N_{Re}$, from the inlet to the position where the maximum velocity is equal to 98% of its fully developed value is defined as the *hydrodynamic entrance length.*

In the boundary layer method, a pair of boundary layers on the inner and outer cylindrical surface of the annulus is assumed to grow from the inlet of the contraction, where the velocity profile is assumed flat, to a position downstream where the two boundary layers merge together. The equations of change describing the fluid motion inside the boundary layers are (Tiu and Bhattacharyya, 1973):

$$\frac{\partial u}{\partial x} + \frac{1}{r}\left(\frac{\partial rv}{\partial r}\right) = 0 \quad \text{(Continuity)} \tag{1}$$

$$\rho\left[u\frac{\partial u}{\partial x} + v\frac{\partial u}{\partial r}\right] = -\frac{\partial p}{\partial x} - \frac{1}{r}\frac{\partial r\tau_{rx}}{\partial r} \quad \text{(Motion)} \tag{2}$$

For power-law fluids, the momentum flux or shear stress distribution in an annulus is represented approximately by

$$\tau_{rx} = -K\left|\frac{du}{dr}\right|^{n-1}\frac{du}{dr} \tag{3}$$

Since the growth of the two boundary layers in an annulus is antisymmetric, the equations of motion must be written separately for each boundary layer. The final differential equations describing the growth of boundary layers with respect to the axial position are given in the previous paper (Tiu and Bhattacharyya, 1973). In the momentum-energy integral technique, the velocity distributions inside the two boundary layers at any axial position in the developing region are assumed to be represented by the Newtonian second-order polynomial function,

$$\frac{u}{U} = 2y - y^2 \tag{4}$$

where the dimensionless radial distance is given by $y = (r - r_1)/\delta_1$ for the inner boundary layer, and $y = (r_2 - r)/\delta_2$ for the outer boundary layer. In the central core region outside the boundary layers the velocity is assumed to be independent of the radial position and equal to the free stream velocity U. The velocity U obtained from the overall mass balance across an annular flow section, in the developing region is

$$U^+ = \frac{U}{\langle u\rangle} = \frac{1-k^2}{\beta^+} \tag{5}$$

where

$$\beta^+ = (1-k^2) + \frac{\delta_2{}^{+2} - \delta_1{}^{+2}}{6} - \frac{2}{3}(k\delta_1{}^+ + \delta_2{}^+) \tag{6}$$

By continuity, the free stream velocity will accelerate from $U = \langle u\rangle$ at the inlet to $U = u_m$ at the point of fully-developed flow.

In the fully developed flow region, Fredrickson and Bird (1958) presented a detailed analysis for power law and Bingham plastics fluids. The local velocity for power-law fluids at any radial position in the fully developed flow region may be obtained by integrating the following expressions:

$$\frac{u}{\langle u\rangle} = \frac{1-k^2}{\Omega_p}\int_k^\xi \left(\frac{\lambda^2}{\xi} - \xi\right)^{1/n} d\xi \qquad k \leq \xi \leq \lambda \tag{7}$$

and

$$\frac{u}{\langle u\rangle} = \frac{1-k^2}{\Omega_p}\int_\xi^1 \left(\xi - \frac{\lambda^2}{\xi}\right)^{1/n} d\xi \qquad \lambda \leq \xi \leq 1 \tag{8}$$

The function Ω_p and the axis of maximum velocity λ are both functions of the flow behavior index n and the annular aspect ratio k. Values of Ω_p, λ, and u_m are tabulated by Fredrickson and Bird (1958).

EXPERIMENT

Developing and fully developed velocity profiles were measured in an abrupt 2 to 1 annular contraction. A detailed description of the flow system is available elsewhere (Bhattacharyya and Tiu, 1974). The geometrical configuration of the experimental set-up was identical to that used for pressure measurements (1974) except that the test section for velocity measurements was made of glass instead of copper. A flow straightener consisting of a bundle of small copper tubes was also inserted at a distance of 38 mm upstream of the contraction in order to generate a uniform entry velocity profile.

Figure 1 shows the details of the entrance section of the annulus following a 2 to 1 contraction. The concentric annulus downstream of the contraction consisted of a 38-mm (1.5 in.) I.D. outer glass tube and a 16-mm (0.625 in.) O.D. inner stainless steel tube. The aspect ratio of the test section was $k = 0.42$. The upstream side of the contraction was another annulus consisting of a 76-mm I.D. glass tube and a 16-mm O.D. stainless steel tube. The entrance joint was constructed by gluing a 0.23-m (9 in.) long piece of perspex tube to the inner surface of the annulus space between the 76-mm and 38-mm tubes using a transparent cellulose caprate optical cement. The outer surface of the perspex tube was held to the glass tube with the aid of four O-rings. The small gap space between the glass and perspex tubes was filled with a viscous silicone oil. The annular space downstream of the perspex section was filled with the same fluid used in the experiment. This minimized the refractive effects and provided an optically clear entrance region for photographic purposes.

A technique employing streak photography was used for measuring point velocities. Mearlite, a synthetic pearl essence supplied by Mearl Corporation, N.Y., was used as tracer particles. The particles were dispersed in the fluid and flowed with the same velocity as the moving fluid. A multiflash slit of light, 0.38 mm wide × 50.8 mm long, together with a continuous light source, coming through an optical assembly box provided illumination of the lower half of the central vertical section of the annulus. An electronic flash delay unit was used to record the time interval between the two flashes for every photograph. The motion of a single tracer particle at any radial position over the time interval was photographically monitored. A 35-mm single reflex Exacta varex camera with 50-mm lens was employed. The entire optical system consisting of the optical assembly box, the viewing box, the camera, and the flash delay unit was mounted on a carriage which could be moved along guide rails to any axial position of the annulus where streak photographs were taken. The exposed films were analyzed on a X-Y Data Reader.

The test fluids employed in the experiment were five aqueous solutions of Methocel 90-HG (hydroxypropyl-methyl-cellulose) and one dilute Separan AP-30 solution (partially hydrolyzed polyacrylamide), both from Dow Chemical. Fundamental fluid properties were characterized in the form of shear stress versus shear rate on an R-16 Weissenberg cone-and-plate rheogoniometer before and after each experimental run.

RESULTS AND DISCUSSION

Shear stress-shear rate data measured for the test fluids were fitted to a power-law fluid model over the shear rate range of interest on the annular flow system. The rheological constants, n and K, for all the test solutions are listed in Table 1. During the course of the experiment no shear degradation was observed for all solutions as indicated from the property measurements before and after each experimental run on the flow system. Furthermore, all Methocel solutions used in the present investigation were considered to be inelastic or purely viscous, since no measurable first normal stress difference was recorded on the Weissenberg rheogoniometer for these fluids in the shear rate and concentration ranges employed. The 0.21% Separan solution was found to exhibit viscoelastic behavior only at very high shear rate, well beyond the present experimental range. Hence, the fluid was also considered to be inelastic for the present purpose.

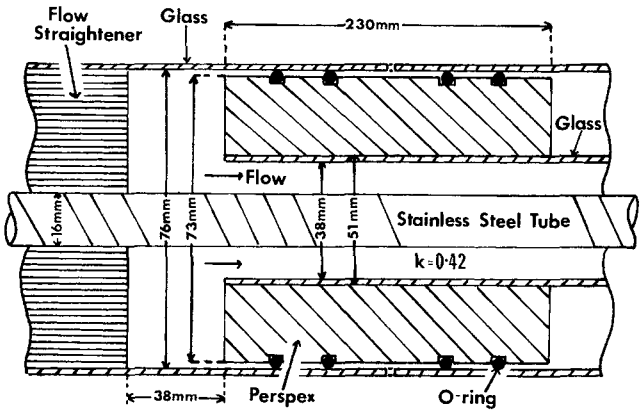

Fig. 1. Details of the glass-perspex joint of the annular contraction.

TABLE 1. RHEOLOGICAL CONSTANTS FOR THE INELASTIC POWER-LAW FLUIDS AND THEIR ENTRANCE LENGTH

Fluid	Concentration, wt. %	n	K ($Ns^n m^{-2}$)	$x_e/r_H N_{Re}$**
Methocel A	0.35	0.815	0.077	0.0414
Methocel B	0.45	0.76	0.12	0.0396
Methocel C	0.51	0.70	0.20	0.0372
Methocel D	0.53	0.685	0.295	0.0369
Methocel F	0.56	0.64	0.52	0.0348
Separan*	0.21	0.53	0.29	0.0282

All rheological constants were measured over a shear rate range of 30 to 1300 s^{-1} and at a temperature of 20 ± 0.5°C.

* First normal stress difference for the 0.21% Separan was very small under the present experimental conditions. Hence, the solution was considered to behave as inelastic fluid.

** Entrance lengths were calculated from the theoretical solution based on the 98% criterion.

Fully Developed Velocity Profiles

Fully developed velocity profiles were measured for all test fluids on the annular flow system over a number of flow rates. The Reynolds numbers employed in the velocity measurements were in the range $112 \leq N_{Re} \leq 1220$. Typical velocity profiles obtained for two inelastic power-law fluids, 0.35% and 0.51% Methocel solutions, are presented in Figures 2 and 3, respectively. The solid curves represented the theoretical solution of Fredrickson and Bird (1958) obtained by numerically integrating Equations (7) and (8). Both figures show excellent agreement between the experimental and theoretical results, with an average deviation of ± 4%. The scattering of data points around the theoretical curves may be attributed mainly to experimental errors. Similar agreements were obtained for all other test fluids. It should be pointed out that in the present flow system it was impractical to measure velocity profiles for Newtonian fluids under laminar flow conditions. Hence, comparisons could not be made with the rigorous theoretical solution for Newtonian flow in annuli. To establish the accuracy of the measurement technique, the average velocity determined from graphical integration of the measured velocity profile was compared to the measured average velocity, $\langle u \rangle = Q/A$. The agreement between the integrated and measured velocities was within ± 5.5% for all fluids. This not only established the measurement technique for velocity profiles in an annulus, but also substantiated the theoretical solution of Fredrickson and Bird, which had never been compared with the velocity profile data before.

The velocity profile for pseudoplastic power-law fluids in an annulus is antisymmetric. The axis of zero shear or maximum velocity, which is a function of flow behavior index n and aspect ratio k, is closer to the inner cylinder of the annulus. For a particular aspect ratio, in the present case $k = 0.42$, the shape of the velocity profile becomes more blunt as n decreases from unity, and approaches a

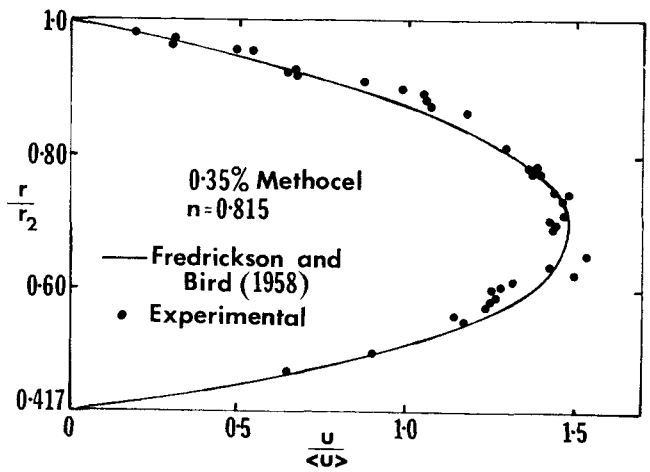

Fig. 2. Fully developed velocity profile for the 0.35% Methocel solution.

flat profile when $n = 0$. This may not be immediately evident from the two profiles shown in Figure 2 and 3 as the n values of the two fluids are relatively close, 0.815 as compared to 0.70.

Developing Velocity Profiles

Local velocities at various axial position in the entrance region of the annulus were measured for all test fluids at several flow rates in the same Reynolds number range employed for fully developed flow measurements. Figure 4 shows four typical developing velocity profiles obtained for the 0.35 % Methocel solution at different axial positions and for $N_{Re} = 695$. The four axial positions shown in the figure correspond to the dimensionless axial distances from the inlet of the contraction: $x/r_H N_{Re} = 0.0065$, 0.0208, 0.039, and 0.0675, respectively. It should be pointed out that in the present set-up accurate velocity data could not be obtained exactly at the inlet plane where $x = 0$. The glass-perspex joint at the contraction was not optically clear to enable distinct photographs of tracer particles to be taken at that location. The nearest position from the inlet where clear velocity profiles could be measured was found to be at a distance about 2 cm downstream of the contraction. It can be observed from Figure 4 that the velocity profile obtained at a distance 2.5 cm from the inlet is relatively flat with a large central core of uniform velocity and a very steep velocity gradient near the walls of the annulus. This implies that the flow is only slightly developed at this position. As the fluid moves further downstream the size of the central core diminishes until the flow becomes fully developed. The solid curves in the figure represent the developing velocity profiles predicted from the momentum-energy integral solution (Tiu and Bhattacharyya, 1973). The velocities inside the inner and outer boundary layers and in the central core region are represented by Equations (4)and (5), respectively. Good agreement can be seen between the experimental and theoretical results. The average deviations between the theory and the experimental for all test fluids and at all axial positions in the entrance region were found to be within ± 5%.

The dimensionless maximum velocity $u_m/\langle u\rangle$, corresponding to the free stream velocity U^+ in the entrance region, is plotted against the axial distance x/D_H for the 0.35% Methocel solution at three Reynolds numbers in Figure 5. As expected, the maximum velocity increases with axial position from the inlet and reaches a constant value at a position sufficiently downstream where the velocity becomes fully developed. The actual distance x required for the velocity development increases with increase in flow rate or Reynolds number. For the 0.35% Methocel solution, values of x/D_H for the maximum velocity to reach 98% of fully developed value, for $N_{Re} = 379$, 695, and 946 were found to be 5.7, 7.8, and 9.8, respectively. Photographic difficulties prevented velocities from being measured at the contraction. The smooth curves drawn through subsequent velocity data points could be extrapolated back to the inlet position at $x/D_H = 0$ which yielded a value of $u_m/\langle u\rangle$ equal to unity. This implies a uniform velocity profile existing at the inlet of the annular contraction, thus verifying the assumption made in the theoretical analysis in which the inlet velocity profile is considered to be flat. In the theoretical analysis, the boundary layers on both inner and outer cylinders were assumed to grow from the point of contraction. However, in view of the extended inner cylinder employed in the present experiment, the actual inner boundary layer would be expected to start growing immediately after the flow straightener. Since the distance between the flow straightener and the contraction is only 38 mm, any predevelopment of boundary layer upstream of the contraction may be ignored.

The data obtained for the maximum velocity as presented in Figure 5 could be brought together into a single plot if the dimensionless distance $x/r_H N_{Re}$ were used. This is demonstrated in Figure 6 where the data obtained for all fluids are plotted in the form of $u_m/\langle u\rangle$ versus $x/r_H N_{Re}$ with n as the parameter. The solid curves represent the predicted axial maximum velocity profiles from the momentum-energy integral solution [Equation (5)]. Ex-

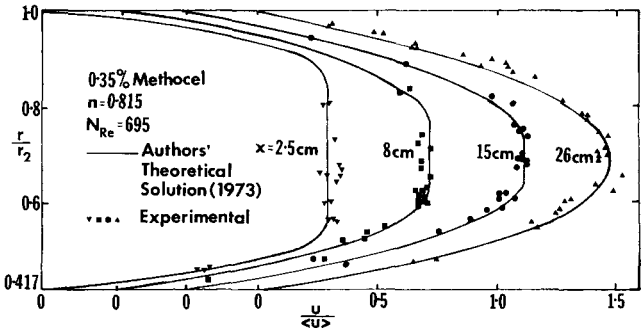

Fig. 4. Developing velocity profiles in the entrance region for the 0.35% Methocel solution.

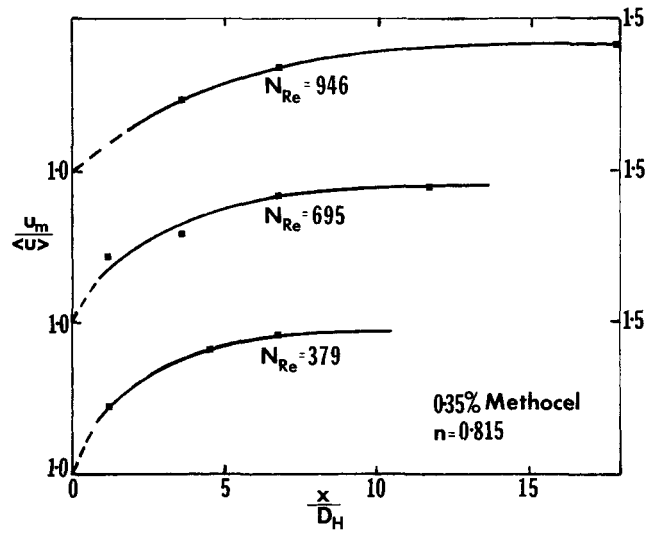

Fig. 5. Dimensionless maximum velocity as function of axial distance x/D_H at various Reynolds numbers for the 0.35% Methocel solution.

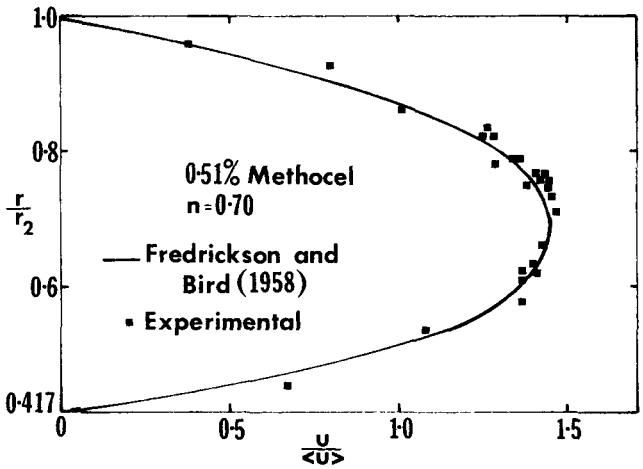

Fig. 3. Fully developed velocity profile for the 0.51% Methocel solution.

cellent agreement between the theoretical and experimental results was obtained for all fluids with an average deviation of about 5%. In view of the experimental errors involved, it is meaningless to try to fit the data empirically by smooth curves and obtain the experimental entrance lengths from these curves. For this reason, the entrance lengths presented were calculated from the theoretical curves as the distances from the inlet to the positions where the dimensionless maximum velocities equal to 98% of their fully developed values. The locus of the entrance lengths calculated for the six inelastic power-law fluids is represented by the broken curve in Figure 6. Values of the entrance length are also tabulated in Table 1. As expected, the entrance length increases with increase in the flow behavior index n. In the limits the broken curve in Figure 6 should extrapolate to zero entrance length for $n = 0$, corresponding to plug flow, and to $x_e/r_H N_{Re} = 0.046$ for $n = 1.0$, the Newtonian case.

Finally a few words must be said concerning the presence of *vena contracta* in the entrance region. In an earlier paper (Bhattacharyya and Tiu, 1974), a *vena contracta* was reported to occur at a short distance downstream of the annular contraction even under laminar flow conditions. This is in contrast with pipe flow of the same contraction ratio where *vena contracta* usually occurs only in turbulent flow (Ramamurthy and Boger, 1971). The presence of *vena contracta* appeared to have significant effects on the axial pressure distribution and hence the loss coefficient. These effects become more pronounced with increasing flow rate or Reynolds number. For this reason the upper limit of N_{Re} employed in the velocity measurements was kept below 1220. Even at $N_{Re} < 1220$ photographs of velocity streamlines revealed certain distortion of flow streamlines toward the inner cylinder of the annulus in the entrance region. It is evident from Figure 4, however, that the distortion appears to have no significant effect on local velocity measurements. This could be due to either (1) the distortion of the streamline was within the experimental error in the velocity measurement, thus making the vena contracts difficult to be observed on the streak photograph; or (2) the tracer particles were confined mostly in the central core region of the flow field, hence any anomaly near the wall could not be detected.

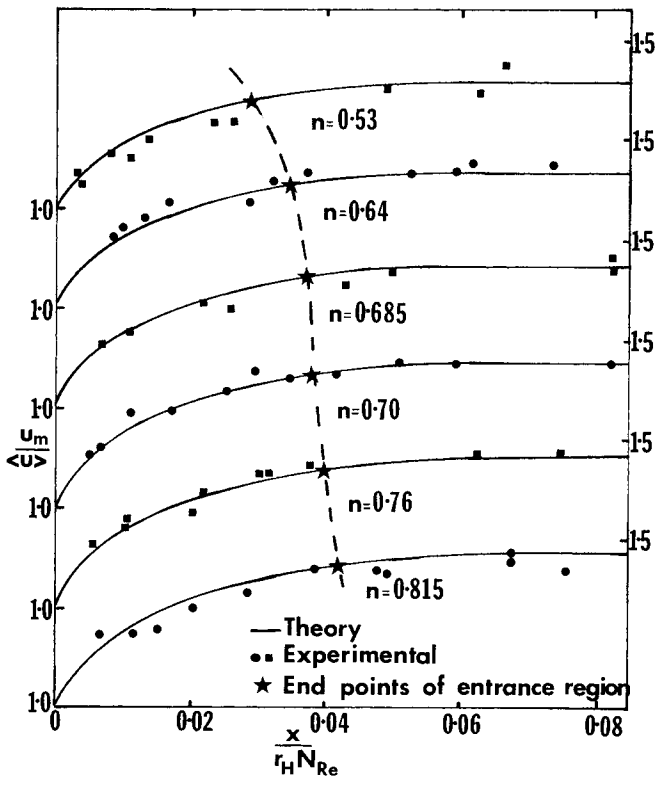

Fig. 6. Dimensionless maximum velocity vs. dimensionless axial distance for all test fluids.

ACKNOWLEDGMENT

The authors wish to acknowledge the financial support of the Australian Research Grant Committee.

NOTATION

D_H = $4r_H$, hydraulic diameter
k = r_1/r_2, aspect ratio of the annulus
K = fluid consistency index for power-law fluid, $Ns^n m^{-2}$
n = flow behavior index for power-law fluid
N_{Re} = Reynolds number for power-law fluid, defined in Tiu and Bhattacharyya (1973)
p = pressure, Nm^{-2}
r = radial position, m
r_1, r_2 = inner and outer radii of the annulus, m
r_H = $r_2(1 - k)/2$, hydraulic radius, m
u = axial velocity, ms^{-1}
u_m = maximum velocity, ms^{-1}
$<u>$ = average velocity, ms^{-1}
U = free stream velocity, ms^{-1}
U^+ = $U/<u>$, dimensionless free stream velocity
v = radial velocity, ms^{-1}
x = axial distance, m
$x/r_H N_{Re}$ = dimensionless axial distance from the inlet contraction
$x_e/r_H N_{Re}$ = dimensionless entrance length
y = $(r - r_1)/\delta_1$ or $(r_2 - r)/\delta_2$ for the inner or outer boundary layer, respectively

Greek Letters

β^+ = function defined by Equation (6)
δ_1, δ_2 = inner and outer boundary layer thicknesses, m
δ_1^+, δ_2^+ = δ_1/r_2, δ_2/r_2, respectively
ξ = r/r_2, dimensionless radial position
λ = dimensionless radial position of maximum velocity
Ω_p = function defined by Fredrickson and Bird (1958)
ρ = density, $kg\ m^{-3}$
τ_{rx} = shear stress, Nm^{-2}

LITERATURE CITED

Bhattacharyya, S., and C. Tiu, "Developing pressure profiles for non-Newtonian flow in an annular duct," *AIChE J.*, **20**, 154 (1974); Bhattacharyya, S., Ph.D. thesis, Monash University, Australia (1974).

Fredrickson, A. G., and R. B. Bird, "Non-Newtonian flow in annuli," *Ind. Eng. Chem.*, **50**, 347 (1958).

Kozicki, W., C. H. Chou, and C. Tiu, "Non-Newtonian flow in ducts of arbitrary cross sectional shape," *Chem. Eng. Sci.*, **21**, 665 (1966).

Kozicki, W., and C. Tiu, "Improved parametric characterization of flow geometries," *Can. J. Chem. Eng.*, **49**, 562 (1971).

McEachern, D. W., "Axial laminar flow of a non-Newtonian fluid in an annulus," *AIChE J.*, **12**, 328 (1966).

RamaMurthy, A. B., and D. V. Boger, "Developing Velocity Profiles on the Downstream Side of a Contraction in Inelastic Polymer Solutions," *Trans. Soc. Rheol.*, **15**, 709 (1971).

Rotem, Z., "Non-Newtonian flow in annuli," *J. Appl. Mech., Trans ASME, Ser. E*, **29**, 421 (1962).

Tiu, C., and S. Bhattacharya, "Flow Behaviour of power law fluids in the entrance region of annuli," *Can. J. Chem. Eng.*, **51**, 47 (1973).

Manuscript received May 16, 1974; revision received and accepted August 9, 1974.